

**Thermodynamic Analysis of Glycerol Steam Reforming for Hydrogen
Production**

Dissertation submitted in partial fulfillment of
the requirements for the
Bachelor of Engineering (Hons)
(Chemical Engineering)

JUNE 2010

Prepared by:

Mohd Hafis Irsyad Bin Mohd Faudzi

Student ID 10375

Supervised by:

AP DR Ye Lwin

Universiti Teknologi PETRONAS

Bandar Seri Iskandar

31750 Tronoh

Perak Darul Ridzuan

CERTIFICATION OF APPROVAL

**Thermodynamic Analysis of Glycerol Steam Reforming for Hydrogen
Production**

by

Mohd Hafis Irsyad Bin Mohd Faudzi

A project dissertation submitted to the

Chemical Engineering Programme

Universiti Teknologi PETRONAS

in partial fulfilment of the requirement for the

BACHELOR OF ENGINEERING (Hons)

(CHEMICAL ENGINEERING)

Approved by,

(AP DR Ye Lwin)

UNIVERSITI TEKNOLOGI PETRONAS

TRONOH, PERAK

JUNE 2010

CERTIFICATION OF ORIGINALITY

This is to certify that I am responsible for the work submitted in this project, that the original work is my own except as specified in the references and acknowledgements, and that the original work contained herein have not been undertaken or done by unspecified sources or persons.

(Mohd Hafis Irsyad Bin Mohd Faudzi)

ABSTRACT

Glycerol is used in many applications including personal care, food, polymer, and pharmaceutical applications. Rapid growth in biodiesel industry is has resulted in an abundance production of glycerol that had led a huge drop in market prices. In this project, thermodynamic analysis of glycerol steam reforming, using the minimization of Gibbs energy has been evaluated. The thermodynamic equilibrium analysis is performed over the following variables range: pressure 1-50 atm, temperature 473-1073K, and water-to-glycerol feed ratio 0-5. The study revealed that the best conditions for producing hydrogen is at a temperature $>973\text{K}$ and a molar ratio of water to glycerol of 5:1.

AKNOWLEDGEMENT

The completion of the Final Year Report benefited from contributions by many, of whom the following deserve special mention. First and foremost, I would like to praise Allah the Almighty, for His guidance and blessings, then I wish to take the opportunity to express my utmost gratitude to the individual that have taken the time and effort to assist me in completing the project. Without the cooperation of these individuals, no doubt I would have faced some minor complications throughout the course.

My deepest gratitude goes to my supervisor Assoc Prof Dr. Ye Lwin for valuable guidance and advice. He inspired me greatly to work in this project. His willingness to motivate me contributed tremendously to the project. I thank him for all the knowledge he had shared and technical professionalism support as well as providing me with all the initial information required to begin the project.

Last but not least, I would like to express my sincere gratitude towards the FYP coordinators, Dr. Khalik Mohamad Sabil and Dr. Mohanad El-Harbawi for providing the assistance and guidelines for the project. They have provided good time management in terms of planning in order to complete all the required tasks within the time frame. Their comments and advice are very useful to us especially when finalizing the project.

Special thanks to Universiti Teknologi PETRONAS for providing me the necessary facilities used in this project. Finally yet importantly, deepest thanks go to all my fellow colleagues, friends and family who have been great inspirations for me to complete the Final Year Project. Without helps of the particular mentioned above, this project would not been successfully completed.

TABLE OF CONTENTS

ABSTRACT	III
AKNOWLEDGEMENT.....	IV
NOMENCLATURE.....	VIII
CHAPTER 1	1
INTRODUCTION.....	1
1.1 BACKGROUND	1
1.2 PROBLEM STATEMENT	2
1.3 OBJECTIVE.....	2
CHAPTER 2	3
LITERATURE REVIEW	3
2.1 HYDROGEN PRODUCTION.....	3
2.2 GLYCEROL STEAM REFORMING	5
2.3 THERMODYNAMIC ANALYSIS	6
CHAPTER 3	11
METHODOLOGY	11
3.1 THEORETICAL BACKGROUND.....	11
3.3 THERMODYNAMIC DATA.....	13
3.4 SOFTWARE.....	13
3.5 METHOD OF CALCULATIONS.....	13
CHAPTER 4	17
RESULT AND DISCUSSION.....	17
4.1 EFFECT OF OPERATING CONDITIONS ON HYDROGEN PRODUCTION	17
4.2 EFFECT OF OPERATING CONDITIONS ON METHANE FORMATION.....	19
4.3 EFFECT OF OPERATING CONDITIONS ON CARBON MONOXIDE AND CARBON DIOXIDE FORMATION	21
4.4 EFFECT OF OPERATING CONDITIONS ON HIGH MOLECULAR-WEIGHT COMPOUNDS FORMATION.....	21
CHAPTER 5	23
CONCLUSION AND RECOMMENDATION	23
APPENDIX A	26
APPENDIX B	27

LIST OF FIGURES

Figure 1: Moles of hydrogen vs temperature at different water to glycerol feed ratio at P = 1 atm.....	19
Figure 2: Molar fraction of hydrogen vs temperature at different water to glycerol feed ratio at P = 1 atm.....	19
Figure 3: Moles of hydrogen at selected pressure and water to glycerol feed ratio = 5:1	19
Figure 4: Moles of methane vs temperature at different water to glycerol feed ratio at P = 1 atm.....	20
Figure 5: Molar fraction of methane vs temperature at different water to glycerol feed ratio at P = 1 atm.....	20
Figure 6: Moles of methane at selected pressure and water to glycerol feed ratio = 5:1	20
Figure 7: Moles of carbon monoxide vs temperature at different water to glycerol feed ratio at P = 1 atm.....	21
Figure 8: Moles of carbon dioxide vs temperature at different water to glycerol feed ratio at P = 1 atm.....	21
Figure 9: Moles of other products vs temperature at different water to glycerol feed ratio at P = 1 atm.....	22

LIST OF TABLES

Table 1: Overall Reaction for Each Model Compound.....	7
Table 2: Enthalpy of Formation and Gibbs Free Energy of Formation	26
Table 3: Physical and Thermodynamic Properties	27

NOMENCLATURE

a_{ij}	Number of gram atoms of element j in a mole of species i
\mathbf{a}_{ij}	Matrix of a_{ij} 's
b_j	Total number of gram atom of element j in the reaction mixture
\hat{f}_i	Fugacity of species i in the gas mixture
f_i°	Fugacity of species i at ties standard state
\bar{G}_i	Gibbs free energy of species i in the gas mixture
G_i°	Gibbs free energy of species i at its standard state
G_i	Gibbs free energy of pure species i at operating conditions
$\Delta G_{f,i}^\circ$	Standard Gibbs free energy of formation of species i
K	Total number of atomic elements
k_{ij}	Binary interaction parameter
N	Total number of species in the reaction mixtures
n_i	Number of moles of species i
nG	Total Gibbs free energy of the system
P	Total pressure of the system
P_c	Critical temperature
R	Gas constant
T	Temperature of the system
T_c	Critical temperature
y_i	Mole fraction of species i
$\hat{\phi}_i$	Fugacity coefficient of species I in the gas mixture
λ_j	Lagrange's multipliers
ω	Acentric factor

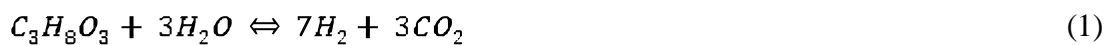
CHAPTER 1

INTRODUCTION

1.1 Background

With its environmental benefits and nationality energy security, the use of biodiesel and its production has gained worldwide momentum [1]. As the result, the world market had been flooded by an overabundance of glycerol. It is necessary to find alternative use for this excess glycerol. One possible route for using glycerol is in hydrogen production. Due to the technical advancements in fuel cell industry, demand for hydrogen is growing [2].

The aim of this project is to analyze the production of hydrogen and other compounds and the effects of the process variables (temperature, pressure, water-to-glycerol ratio of reactants). Overall, the reaction of glycerol steam reforming can be given as follows:



The equilibrium concentrations of different compounds were calculated by a direct minimization G.

1.2 Problem Statement

In order to understand the effects of the process variables, such as system pressure, temperature, and ratio of reactants on steam reforming of glycerol, a complete thermodynamic analysis need to be performed.

For this project, ideal reaction conditions for the steam reforming reaction of glycerol to maximize the yield of hydrogen and minimize undesirable products need to be determined.

1.3 Objective

The objectives of this project are as follow:

1. To carry out detailed thermodynamic analysis of steam reforming of glycerol
2. To find optimum condition for glycerol reforming to get
 - i. maximum yield of hydrogen production
 - ii. maximum conversion of glycerol
 - iii. minimum production carbon monoxide

The main objective is to find the set of n_i 's which can minimize the value of G.

1.4 Scope of Study

This analysis will be performed for the following variables range: pressure 1-5 atm, temperature 473-1073K, and water-to-glycerol feed ratio 1-5.

The species that are considered in this project are: Glycerol ($C_3H_8O_3$), Water (H_2O), Carbon Monoxide (CO), Carbon Dioxide (CO_2), Hydrogen (H_2), Methane (CH_4), Methanol (CH_3OH), Ethane (C_2H_6), Ethanol (C_2H_5OH), Ethylene Glycol ($C_2H_6O_2$), Acetol ($C_3H_6O_2$), Propane (C_3H_8), Propanol (C_3H_7OH), Propylene Glycol ($C_3H_8O_2$), Ethene (C_2H_4), Acrolein (C_3H_4O).

CHAPTER 2

LITERATURE REVIEW

2.1 Hydrogen Production

Hydrogen has the highest energy content of any common fuel by weight, but the lowest energy content by volume. Like electricity, hydrogen is an energy carrier and produced from other substances such as water, fossil fuels, and biomass and also a by-product from other chemical process. But unlike electricity, large quantities of hydrogen can be easily stored and later be used in the future. In addition, it can also be applied in places where it is hard to produce electricity, such as in rural area. It can store the energy until it is required and can also be moved to where it is needed conveniently [3]. Several processes of producing hydrogen are as follows [4]:

1. **Natural Gas Reforming.** Hydrogen can be produced from methane in natural gas using high-temperature steam. This process is called steam methane reforming. Another method, called partial oxidation, produces hydrogen by burning methane in air. Both steam reforming and partial oxidation produce a “synthesis gas,” which is reacted with water to produce more hydrogen.
2. **Renewable electrolysis.** Electrolysis uses an electric current to split water into hydrogen and oxygen.
3. **Gasification.** Process in which coal or biomass is converted into gaseous components by applying heat under pressure and in the presence of steam. A subsequent series of chemical reaction produces a synthesis gas, which is

reacted with steam to produce more hydrogen that then can be separated and purified.

4. **Renewable liquid reforming.** Biomass can also be processed to make renewable liquids fuels that are relatively convenient to transport and can be reacted with high-temperature steam to produce hydrogen at or near the point of end-use.
5. **Nuclear high-temperature electrolysis.** Heat from nuclear reactor can be used to improve the efficiency of water electrolysis to produce hydrogen. Increasing the temperature of water will decrease the amount of electricity required to split it into hydrogen and oxygen, reducing the total energy required.
6. **High-temperature thermochemical water-splitting.** Method of water-splitting using high temperature generated by solar concentrators (special lenses that focus and intensify sunlight) or nuclear reactors to drive a series of chemical reactions that split water. All of the chemical used are recycled within the process.
7. **Photobiological and photoelectrochemical.** When certain microbes consume water in the presence of sunlight, hydrogen is produced as a byproduct of their natural metabolic process. Using a similar concept, photoelectrochemical systems produce hydrogen from water using special semiconductors and energy from sunlight.

Steam reforming of glycerol is the most commonly used among all others process of producing hydrogen.

2.2 Glycerol Steam Reforming

Several research and study had been focused on developing new glycerol platform chemistry and possible product to take advantages of a material that increasingly cheap and abundant. At the 232nd National Meeting of the ACS in San Francisco, researchers described various approaches to utilizing glycerol ($C_3H_8O_3$) as a feedstock for different fuel outcomes: a low-temperature catalytic approach to using glycerol as a source for fuel and chemicals; the steam reformation of glycerol to produce hydrogen; and glycerol as a feedstock for microbial hydrogen production [5].

However, the crude glycerol produced from production of biodiesel had low quality and low economic value. The impurities make it of low quality [6]. Due to its high impurities, it is expensive to purify and use in food, pharmaceutical, and cosmetics industries. Furthermore, even though crude glycerol is useful to burn as a fuel if blended with fuel oil, it will have a serious environmental threat [7].

Steam reforming is one of the alternatives use of crude glycerol that is economically and environmentally friendly. This method is most commonly used and least expensive of producing commercial bulk hydrogen. In this method, steam reacts with hydrocarbons at high temperature (700-100°C) and in the presence of a catalyst to yield hydrogen and carbon monoxide. Carbon monoxide is then subjected to the water-gas shift (WGS) reaction to produce more hydrogen [6].

Therefore, glycerol steam reforming is a viable alternative use for glycerol and potentially a better option than purification [7]. Therefore, thermodynamic analysis is important in order to get more information about the process.

2.3 Thermodynamic Analysis

Thermodynamics is the theory of the relations between heat and mechanical energy, and of the conversion of either into the other. In simpler terms, thermodynamics is the science that tells us which minerals or mineral assemblages will be stable under different conditions. In practical terms, thermodynamics allows us to predict what minerals will form at different conditions (forward modeling).

Thermodynamic studies can provide information on conditions that are conducive for production of hydrogen. The yield of hydrogen depends on several process variables, such as system pressure, temperature and ratio of reactants [8]. Several thermodynamic analyses had been conducted by other researcher not only for the steam reforming of steam reforming of glycerol to produce hydrogen, but also steam reforming of other compound.

2.3.1 Thermodynamics Analysis of Hydrogen Production via Steam Reforming of Bio-Oil Components [9]

The model compounds in Vagia's and Lemonidou's work are acetic acid, ethylene glycol and acetone that represent the major classes of components present in the aqueous fraction of bio-oil. The equilibrium product compositions were investigated in a broad range of conditions like temperature (400–1300 K), steam to fuel ratio (1–9) and pressure (1–20 atm). Thermal decomposition of the bio-oil components is found to be thermodynamically feasible, forming a mixture containing C(s), CH₄, H₂, CO, CO₂, and H₂O at various proportions depending on the specific nature of the compound and the temperature. The overall reaction for each model compounds is as shown in **Table 1** below:

Table 1: Overall Reaction for Each Model Compound

Compound	Overall reforming reactions	ΔH_{298} (Kcal/mol)	ΔG_{298} (Kcal/mol)
Acetic Acid	$C_2H_4O_2 + 2H_2O \rightarrow 2CO_2 + 4H_2$	32.21	10.18
Acetone	$C_3H_6O + 5H_2O \rightarrow 3CO_2 + 8H_2$	58.62	26.89
Ethylene Glycol	$C_2H_6O_2 + 2H_2O \rightarrow 2CO_2 + 5H_2$	21.23	-7.12

From their work, they found that bio-oil components are easily reformed even at low temperatures forming a mixture of hydrogen, carbon monoxide, carbon dioxide and methane with varying composition. Temperature, steam to fuel ratio and pressure are the operating variables which affect to a great extent the equilibrium composition. Increase in temperature up to 900 K favors the formation of hydrogen where maximum concentration of hydrogen is attained. The amount of steam to the inlet mixture determines to a great extent the hydrogen yield. The higher is the steam to fuel ratio the higher is the hydrogen concentration. Best results concerning hydrogen yield are attained at atmospheric pressure.

Carbon free operation is possible at temperatures higher than 600 K and steam to fuel higher than 4 for acetic acid and ethylene glycol and higher than 6 for acetone. Methane is a major product at low temperatures minimizing at 900 K. Carbon monoxide and carbon dioxide are also components of the equilibrium mixture with their concentrations determined by the water gas shift equilibrium. The equilibrium composition under the various operating conditions does not differ significantly among the three model compounds.

2.3.2 Thermodynamics Analysis of Hydrogen Production via Steam Reforming of Dimethyl Ether [10]

Steam reforming of dimethyl ether is a two-step reaction, namely, hydrolysis of dimethyl ether to methanol (Eq. (4)), followed by steam reforming of methanol (Eq. (5)).



In Faungnawakij et al work, the thermodynamic equilibrium of dimethyl ether steam reforming was studied by Gibbs free minimization for carbon formation boundary, dimethyl ether conversion and hydrogen yield in an external reformer. Effect of steam-to-carbon ratio ($S/C = 0-5$) and reforming temperature ($25-1000\text{ }^\circ\text{C}$) and product basis species were investigated. Major gas species involved in the dimethyl ether steam reforming are CH_3OCH_3 , CH_3OH , H_2O , H_2 , CO , CO_2 , CH_4 and coke.

Their results indicated that carbon formation could be avoided by increasing the steam-to-dimethyl ether ratio and/or by increasing the reforming temperature. Based on the compound basis set dimethyl ether, methanol, CO_2 , CO , H_2 , H_2O and coke, complete conversion of dimethyl ether and hydrogen yield above 78% were achieved in the coke-free region at the normal operating temperature of $600\text{ }^\circ\text{C}$ for molten carbonate fuel cell and that of $900\text{ }^\circ\text{C}$ for solid oxide fuel cell. When methane was taken into account, coke formation was significantly suppressed. Hydrogen yield up to almost 100% could be achieved at $S/C > 2$ and $T_r = 125-250\text{ }^\circ\text{C}$ when coke and methane were thermodynamically unfavorable.

2.3.3 Thermodynamics Analysis of Hydrogen Production via Steam Reforming of Methanol [11]

Thermodynamic equilibrium of methanol steam reforming was studied by Gibbs free minimization for hydrogen production as a function of steam-to-carbon ratio ($S/C = 0-10$), reforming temperature ($25-1000\text{ }^\circ\text{C}$), pressure ($0.5-3\text{ atm}$), and product species. The chemical species considered were methanol, water, hydrogen, carbon

dioxide, carbon monoxide, carbon (graphite), methane, ethane, propane, i-butane, n-butane, ethanol, propanol, i-butanol, n-butanol, and dimethyl ether. Coke-formed and coke-free regions were also determined as a function of S/C ratio.

Based upon a compound basis set MeOH, CO₂, CO, H₂ and H₂O, complete conversion of MeOH was attained at S/C = 1 when the temperature was higher than 200 °C at atmospheric pressure. The concentration and yield of hydrogen could be achieved at almost 75% on a dry basis and 100%, respectively. From the reforming efficiency, the operating condition was optimized for the temperature range of 100–225 °C, S/C range of 1.5–3, and pressure at 1 atm.

From their calculation, they found that the reforming condition required from sufficient CO concentration (<10 ppm) for polymer electrolyte fuel cell application is too severe for the existing catalysts (Tr = 50 °C and S/C = 4–5). Only methane and coke thermodynamically coexist with H₂O, H₂, CO, and CO₂, while C₂H₆, C₃H₈, i-C₄H₁₀, n-C₄H₁₀, CH₃OH, C₂H₅OH, C₃H₇OH, i-C₄H₉OH, n-C₄H₉OH, and C₂H₆O were suppressed at essentially zero. The temperatures for coke-free region decreased with increase in S/C ratios. The impact of pressure was negligible upon the complete conversion of MeOH.

2.3.4 Thermodynamics Analysis of Hydrogen Production via Steam Reforming of Ethanol [12]

In this paper, Silva et al had done a thermodynamic analysis of ethanol/water system, using the Gibbs energy minimization method. A mathematical relationship between Lagrange's multipliers and carbon activity in the gas phase was deduced. From this, it was possible to calculate carbon activities in both stable and metastable systems.

For the system that corresponds to ethanol steam reforming at very low contact times, composed mainly of ethylene and acetaldehyde, carbon activities were always much greater than unity over the whole temperature range, changing from 1.2×10^7 at 400 K to 1.1×10^4 at 1200 K. Furthermore, there was practically no effect of the inlet steam/ethanol ratio on carbon activity values. These results indicate that such a system is highly favorable to carbon formation.

On the other hand, by considering a more stable system, in order to represent high contact times, it was observed that carbon activities are much lower and depend greatly on the inlet steam/ethanol ratio employed. Besides, the complete conversion of ethylene and acetaldehyde into other species, such as CO, CO₂, CH₄ and H₂, lowers the total Gibbs energy of the system. By computing carbon activities in experimental systems, it was also possible to explain deviations between thermodynamic analysis and experimental results regarding carbon deposition.

CHAPTER 3

METHODOLOGY

3.1 Theoretical Background

In steam reforming of glycerol, there is two main reactions which can occur in a high temperature steam/fuel mixture: steam reforming and pyrolysis [6]. However many reactions occur simultaneously including many side reactions. The reaction involved in the process is as follows [13]:

Formation of light components:



Formation of heavy components:





The equilibrium composition is calculated through the minimization of Gibbs free energy function of the system [14] given by:

$$nG = \sum_{i=1}^N n_i \bar{G}_i = \sum n_i \Delta G_i^\circ + RT \sum n_i \ln \frac{\hat{f}_i}{f_i^\circ} \quad (19)$$

For gas phase reaction, $\hat{f}_i = \hat{\phi}_i y_i P$. Since the standard state is taken as the pure ideal gas state at 1 bar (100 kPa), $f_i^\circ = 1$ bar. And since the value of G_i° is set equal to zero for each chemical element in the standard state, $G_i^\circ = G_{f_i}^\circ$ for each component.

Substituting these into equation (19) gives:

$$nG = \sum n_i \Delta G_{f_i}^\circ + \sum n_i RT \ln \phi + \sum n_i RT \ln y_i \quad (20)$$

In this project, the set of n_i which minimizes nG at constant T and P , subject to the constraints elemental balances:

$$\sum_{i=1}^N n_i a_{ij} = b_j, \quad j = 1, 2, \dots, K \quad (21)$$

Non-stoichiometric approach is considered in the analysis due to the advantages over the stoichiometric approach in the Gibbs free energy minimization as follows [8]:

1. a selection of the possible set of reactions is not necessary
2. no divergence occurs during the computation
3. an accurate estimation of the initial equilibrium composition is not necessary

3.3 Thermodynamic Data

The Gibbs free energy of formation for the species is calculated from the Gibbs-Helmholtz relation:

$$G = H - TS \quad (22)$$

Where,

$$H = H^{298} + \int_{T_{298}}^T C_p dT \quad (23)$$

$$S = S^{298} + \int_{T_{298}}^T \frac{C_p}{T} dt \quad (24)$$

$$C_p = a + bT + cT^2 \quad (25)$$

3.4 Software

The nonlinear programming model, comprising objective function (20) and the constraints (21), is solved by using MATLAB software. As entry data, the program needs temperature, pressure, number of compounds, number of atoms, values of the Gibbs free energy of formation, and initial guesses for n_i 's in the equilibrium. The temperature, pressure, and ratio of reactants against the production of the considered products are plotted to see the effects. The thermodynamic data for the calculation is obtained from thermodynamic books [15, 16 and 17] and Aspen Tech HYSYS. The data used in this study is summarized in the table in **Appendix A**.

3.5 Method of Calculations

The problem can be solved by using Lagrange multiplier method in the model (20)-(21). To solve the problem using MATLAB as shown in **Appendix B**, the chemical identities, starting moles, temperature, and pressure of the system, atomic matrix \mathbf{a}_{ij} , critical constants (T_c , P_c , ω) and the ideal gas standard Gibbs free energy of formation of each species at T , binary interaction parameters (k_{ij}), and initial estimates of moles of components and compressibility factor (Z) of the mixture need

to be supplied. The initial estimate for Z is unity. MATLAB will calculate chemical equilibrium occurring in both ideal gas phase and non-ideal gas phase system.

3.5.1 Fugacity Coefficient Calculation Using Soave-Redlich-Kwong Equation of State

For calculation using real gas, SRK equation of state is used. The fugacity coefficient of each species in the mixture is calculated using the Soave-Redlich-Kwong (SRK) equation of state [18]. Finally, the Gibbs function of the system, the left-hand side of equation (20), is computed.

The fugacity coefficients are calculated using equation (26) where Z is given by S-R-K equation of state using equation (27). The parameters A, B, B_i , $(a\alpha)_{ij}$, and $a\alpha$ of these equation are calculated from equation (28) to equation (37).

$$\ln \hat{\phi}_i = \frac{B_i}{B} (Z - 1) - \ln(Z - B) + \frac{A}{B} \left[\frac{B_i}{B} - \frac{2}{a\alpha} \sum_j y_j (a\alpha)_{ij} \right] \ln \left(1 + \frac{B}{Z} \right) \quad (26)$$

$$f(Z) = Z^3 - Z^2 + (A - B - B^2)Z - AB = 0 \quad (27)$$

$$A = (a\alpha)P/R^2T^2 \quad (28)$$

$$B = bP/RT \quad (29)$$

$$B_i = b_iP/RT \quad (30)$$

$$a\alpha = \sum_i \sum_j y_i y_j (a\alpha)_{ij} \quad (31)$$

$$b = \sum y_i b_i \quad (32)$$

$$(a\alpha)_{ij} = (1 - k_{ij}) \sqrt{(a\alpha)_i (a\alpha)_j} \quad (33)$$

$$(a\alpha)_i = a_i \alpha_i \quad (34)$$

$$a_i = 0.42747R^2T_{ci}^2/P_{ci} \quad (35)$$

$$b_i = 0.08664RT_{ci}/P_{ci} \quad (36)$$

$$\alpha_i = [1 + (0.480 + 1.574\omega_i - 0.176\omega_i^2)(1 - T_{ri}^{0.5})]^2 \quad (37)$$

3.5.2 Gibbs Free Energy of Formation

The equation for $\Delta G_{f,i}^0$ in equation (20) is derived from equation as follows:

$$\Delta G_{f,i}^0 = a + bT + cT^2 + dT^3 + eT^4 + fT^5 \quad (38)$$

Where,

A, b, c, d, e = constant

3.5.3 Binary Interaction Parameter, kij [17]

The binary parameter is used in equation (33). For molecules which do not differ greatly in size or chemical structure the binary constant kij can be set equal to zero. Tarakad and Danner have also given guidelines for the estimation of kij. For binaries where both components fall into one of these categories (hydrocarbon, rare gases, permanent gases, carbon monoxide, perhalocarbons, kij may be calculated by:

$$k_{ij} = 1 - \frac{8(r_{ci}r_{cj})^{1/2}}{(v_{ci}^{1/8} + v_{cj}^{1/8})^8} \quad (39)$$

Where,

Vc = critical volume

3.5.4 Acentric Factor, ω [17]

The acentric factor used in equation (37) is calculated using the following formula.

$$w = \frac{3}{7} \frac{\theta}{1-\theta} \log P_c - 1 \quad (40)$$

Where,

$$\theta = T_b/T_c$$

T_b = boiling point temperature

T_c = critical temperature

P_c = critical pressure

CHAPTER 4

RESULT AND DISCUSSION

Production of hydrogen and other compounds at different temperatures, WGFRs, and pressures has been analyzed. The steam reforming of glycerol produces H₂, CH₄, CO, and CO₂ together with the unreacted water and glycerol. Methane competes against H₂ but not a desirable product in the case of hydrogen production while oxygenated compounds carbon monoxide and carbon dioxide is considered impurities because they do not compete against H₂. The conversion of glycerol was always greater than 99.99%, over the temperature, pressure, and WGFR ranges analyzed. The conversion can be considered complete.

4.1 Effect of Operating Conditions on Hydrogen Production

Figure 1 shows the hydrogen moles and molar fractions at different temperatures and WGFRs. As can be seen, the number of moles of hydrogen increases with increasing temperature. Since the reaction of steam reforming of glycerol is an endothermic reaction, according to the Le-chatelier's principle, an increase in temperature favors the reaction to occur in the forward direction. Therefore, the reaction will produce more hydrogen and carbon dioxide as the temperature increase as shown in the following equation:



The upper limit of the moles of hydrogen produced per mole of glycerol is 5.37 at 973 K, WGFR=5:1, and P =1 atm vs the stoichiometric value of 7. At higher WGFRs, i.e., 5:1 and 4:1, the number of moles of hydrogen produced at 1073K is lower than in 973K. The number of moles of hydrogen is at its maximum at 973K

and decreases thereafter in both cases. A similar observation was made by Semelsberger and Borup [19] in dimethyl ether steam reforming. Moles of hydrogen decrease together with CO₂ at temperatures >973 K, but at the same time, moles of CO and water increase. Perhaps, this can be explained by the following equation:



Figure 2 shows the hydrogen molar fraction at different temperatures and WGFRs. Same as the mole of hydrogen, the mole fraction of moles of hydrogen increases with increasing temperature. Furthermore, the molar fraction of hydrogen is found to be higher at low WGFRs. This is because of the significant amount of water present in the product at high WGFRs. The unreacted water in the product reduces the molar fraction of hydrogen but not necessarily the quantity. Even though the greatest quantity of hydrogen is produced at excess water at all temperatures, it can only be the best conditions if the purification problems can be overcome.

Figure 3 shows the number of moles of hydrogen as pressure increase. The effect of the pressure on the glycerol steam reforming process is found to be consistent with methanol and ethanol steam reforming processes [20, 21 and 22]. This can be explained by Le-chatelier's principle where the position of equilibrium moves in such a way as to tend to undo the change made. When the pressure increase, the position of equilibrium will move in such a way as to decrease the pressure again - if that is possible. It can do this by favoring the reaction which produces the fewer molecules. Since there are 10 molecules in the right side and only 4 molecules in the left side of equation (41), the reaction will favor the left side of the equation, producing less hydrogen as the pressure increase.

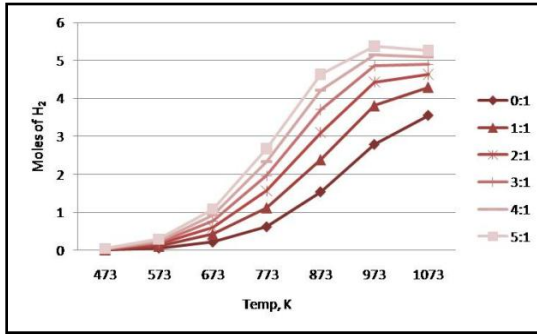


Figure 1: Moles of hydrogen vs. temperature at different water to glycerol feed ratio at P = 1 atm

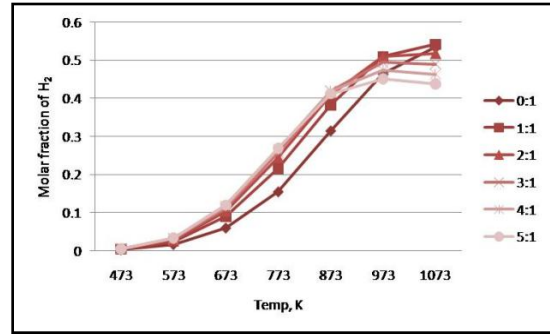


Figure 2: Molar fraction of hydrogen vs. temperature at different water to glycerol feed ratio at P = 1 atm

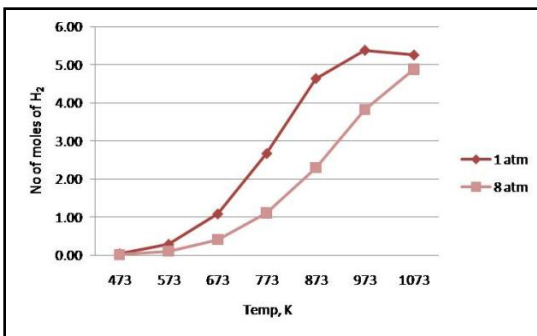


Figure 3: Moles of hydrogen at selected pressure and water to glycerol ratio = 5:1

4.2 Effect of Operating Conditions on Methane Formation

Figure 4 shows the moles of methane as a function of temperature. Methane production decreases when the temperature and the WGFR increase. At higher WGFRs, i.e., 5:1 and 4:1, and at higher temperatures (>973K), the formation of methane is almost inhibited. As the temperature increases, moles of water and CH₄ decrease with increasing CO, CO₂, and H₂. This can be attributed to the methane steam reaction to produce CO or CO₂ and H₂ as given by equations below [20]:



Figure 5 shows molar fraction of methane as a function of temperature. Molar fraction of methane decreases with the increase in temperature and WGFR. Although, methane formation is low at low WGFR, the molar fraction is higher than other feed ratios analyzed in the study. As can be seen from **Figure 5**, as we increase temperature and WGFR, mole fraction of CH_4 decreases.

Figure 6 shows the number of moles of methane as pressure increase. Higher pressure favors the formation of methane. This can also be explained by Le-chatelier's principle, where from equation (43) and equation (44), the reaction will favor the left hand side of the reaction in order to undo the change of increasing the pressure.

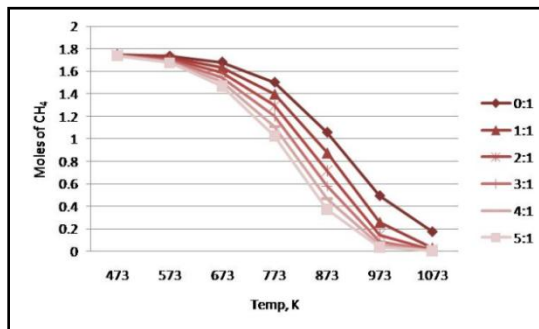


Figure 4: Moles of methane vs. temperature at different water to glycerol feed ratio at $P = 1 \text{ atm}$

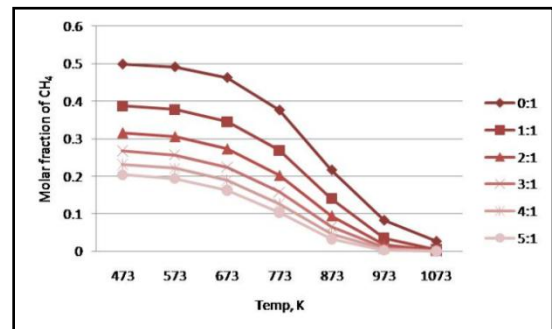


Figure 5: Molar fraction of methane vs. temperature at different water to glycerol feed ratio at $P = 1 \text{ atm}$

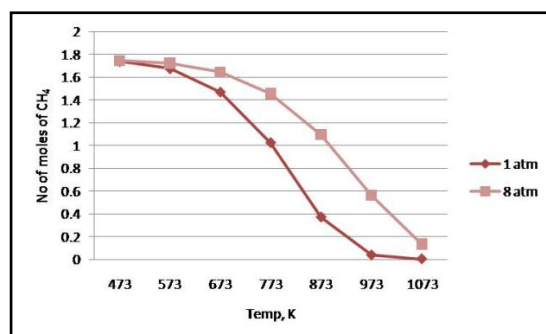


Figure 6: Moles of methane at selected pressure and water to glycerol ratio = 5:1

4.3 Effect of Operating Conditions on Carbon Monoxide and Carbon Dioxide Formation

Figure 7 and Figure 8 shows the number of moles of CO and CO₂ respectively at different temperatures under selected WGFRs. Number of moles of CO increases with the increase in temperature but decreases with the increasing WGFR. However, the number of moles of CO₂ increases with increasing temperature, goes through maximum at around 773 K, and then decreases at higher temperatures. This behavior may be attributed to the reformation of CH₄ with CO₂ by the flowing reaction [20]:

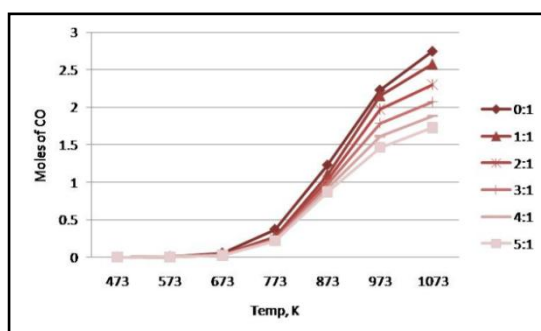


Figure 7: Moles of carbon monoxide vs. temperature at different water to glycerol feed ratio at P = 1 atm

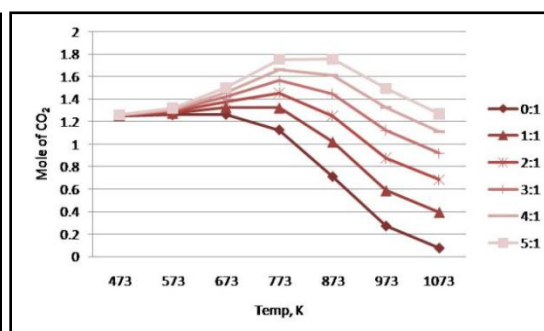


Figure 8: Moles of carbon dioxide vs. temperature at different water to glycerol feed ratio at P = 1 atm

4.4 Effect of Operating Conditions on High Molecular-Weight Compounds Formation

Figure 9 shows the moles of other products at different temperature and water to glycerol feed ration. Through this study, it was found that the formation of this high molecular-weight compounds are negligible and only the primary products of steam reforming – glycerol, water, CO, CO₂, and H₂ – are dominant, in spite of the fact that the glycerol steam reforming is highly endothermic and the formation of some high molecular-weight compounds from glycerol is thermodynamically favorable. This can be summarized in the Table 2 below:

Table 2: Enthalpy of Formation and Gibbs Free Energy of Formation

Reaction	ΔH_{298}° kJ mol ⁻¹	ΔG_{298}° kJ mol ⁻¹
$C_3H_8O_3 + 3H_2O = 7H_2 + 3CO_2$	127	-49
$C_3H_8O_3 = C_3H_6O_2 + H_2O$	-25.03	-65.13
$C_3H_6O_2 + H_2 = C_3H_8O_2$	-67.00	-19.44
$C_3H_8O_2 + H_2 = C_2H_6O_2 + CH_4$	-7.50	-42.62
$C_3H_8O_3 = 4H_2 + 3CO$	251.21	36.89
$CO + H_2O = CO_2 + H_2$	-41.16	-28.62

The possible reason is that the glycerol molecule is highly ordered in nature, while the low molecular-weight gases are highly disordered. According to the law of disorder where natural tendency is for systems to move to the direction of maximum disorder, not vice-versa. Therefore, this indicates that in the presence of suitably selective catalysts, the glycerol is a favorable feedstock for production of a wide range of hydrocarbons. Another reason is that according to **Table 2**, the high molecular weight component is exothermic reaction. The reaction is favorable at low temperature but not detected in the temperature of the study range.

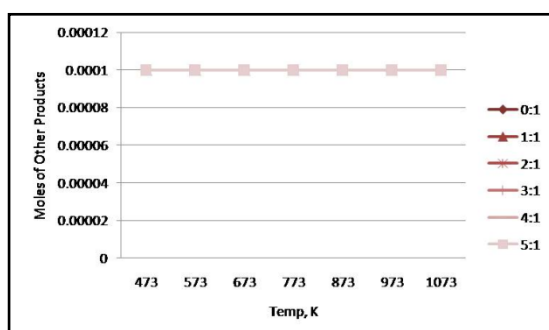


Figure 9: Moles of other products vs. temperature at different water to glycerol feed ratios at P = 1 atm

CHAPTER 5

CONCLUSION AND RECOMMENDATION

A thermodynamic analysis for hydrogen production by steam reforming of glycerol has been performed. The number of moles of hydrogen produced is calculated based on minimizing the Gibbs free energy. From the result, it shows that at high temperatures, low pressures, and high water to glycerol feed ratios favor the hydrogen production. The study revealed that the best conditions for producing hydrogen is at a temperature $>973\text{K}$ and a molar ratio of water to glycerol of 5:1. Under these conditions methane production is minimized, and carbon formation is thermodynamically inhibited. The upper limit of the moles of hydrogen produced per mole of glycerol is 5.37 vs. the stoichiometric limit of 7. Although water-rich feed increases the hydrogen production, a significant amount of unreacted water is resulted in the products. The behavior of this system is very similar to that of steam reforming of ethanol.

Form this project, glycerol steam reforming is found to be not equilibrium-limited for all conditions considered. For aqueous reforming region (high pressure and low temperature), the liquid-phase non-ideality and the vapor-liquid phase equilibrium should be included in the calculations. It should be realized that the calculation data may deviate from the experiment. Reaction mechanisms, i.e. kinetic control or heat and mass transfer control, would also affect the result of glycerol steam reforming in practical applications.

REFERENCES

- [1] Thompson JC, He BB. Characterization of crude glycerol from biodiesel production from multiple feedstocks. *Appl Eng Agric* 2006; 22(2):261–5.
- [2] Dunn S. Hydrogen futures: toward a sustainable energy system. *Int J Hydrogen Energy* 2002;27:235–64.
- [3] Energy Information Administration, *Alternatives to Traditional Transportation Fuels 2006*, U.S. Department of Energy, Washington, DC May 2008.
- [4] Hydrogen Program, Hydrogen Production, U.S. Department of Energy, Washington, DC November 2008.
- [5] Millikin, M. 13 September 2006
http://www.greencarcongress.com/2006/09/pathways_for_gl.html.
- [6] Matthew Slinn, Kevin Kendall, Christian Mallon and James Andrews (2008), Steam reforming of biodiesel by-product to make renewable hydrogen, *Bioresource Technology* **99**, pp. 5851-5858.
- [7] Joshi, Manoj. 2009, Feasibility Analysis of Steam Reforming Of Biodiesel By-Product Glycerol To Make Hydrogen, Senior Scholar Thesis, Texas A&M University, Texas.
- [8] Sushil Adhikari, Sandun Fernando, Steven R. Gwaltney, S.D. Filip To, R. Mark Bricka (2007). A thermodynamic analysis of hydrogen production by steam reforming of glycerol, *Hydrogen Energy* **32**; 2875 – 2880.
- [9] Vagia E.Ch., Lemonidou A.A. (2007) Thermodynamic analysis of hydrogen production via steam reforming of selected components of aqueous bio-oil fraction *International Journal of, Hydrogen Energy* **32 (2)**, pp. 212-223.
- [10] Faungnawakij K., Kikuchi R., Eguchi K (2007) Thermodynamic analysis of carbon formation boundary and reforming performance for steam reforming of dimethyl ether, *Journal of Power Sources*, **164 (1)**, pp. 73-79.
- [11] Faungnawakij K., Kikuchi R., Eguchi K. (2006) Thermodynamic evaluation of methanol steam reforming for hydrogen production, *Journal of Power Sources*, **161 (1)**, pp. 87-94.

- [12] Aline Lima da Silva (2009), Célia de Fraga Malfatti, and Iduvirges Lourdes Müller, Thermodynamic analysis of ethanol steam reforming using Gibbs energy minimization method: A detailed study of the conditions of carbon deposition, *Int. J. Engng Ed.* 34, 4321-4330.
- [13] D. Sutton, B. Kelleher and J. Ross, Review of literature on catalysts for biomass gasification, *Fuel Processing Technology* **73** (3) (2001), pp. 155–173.
- [14] Y. Lwin (2000.), Chemical equilibrium by Gibbs energy minimization on spreadsheet, *Int. J. Engng Ed.* Vol. 16, No. 4, pp. 335-339.
- [15] Carl L. Yaws, The Yaws handbook of thermodynamic properties for hydrocarbons and chemicals.
- [16] Carl L. Yaws, The Yaws handbook of physical properties for hydrocarbons and chemicals.
- [17] Reid Robert C, Prausnitz John M, Poling Bruce E. (Eds.). (1988). *The properties of gases and liquids* (4th ed.). Singapore, McGraw-Hill Book Co
- [18] G. Soave, Equilibrium constants form a modified Redlich-Kwong equation of state, *Chem. Eng. Sci.*, **27**, (1972) pp. 1197-1203.
- [19] Semelsberger TA, Borup RL. Thermodynamic equilibrium calculations of hydrogen production from the combined processes of dimethyl ether steam reforming and partial oxidation. *J Power Sources* 2006;155: 340–52.
- [20] Amphlett JC, Evans MJ, Jones RA, Mann RF, Weir RD. Hydrogen production by the catalytic steam reforming of methanol part 1: the thermodynamics. *Can J Chem Eng* 1981; 59:720–7.
- [21] García EY, Laborde MA. Hydrogen production by the steam reforming of ethanol: thermodynamic analysis. *Int J Hydrogen Energy* 1991; 16(4):307–12.
- [22] Vasudeva K, Mitra N, Umasankar P, Dhingra SC. Steam reforming of ethanol for hydrogen production: thermodynamic analysis. *Int J Hydrogen Energy* 1996;21(1):13–8.

APPENDIX A

Table 3: Physical and Thermodynamic Properties

	C3H8O3	H2O	CO	CO2	H2	CH4	CH3OH	C2H6	C2H5OH	C2H6O2	C3H6O2	C3H8	C3H7OH	C3H8O2	C2H4	C3H4O
Critical Temperature, TC,K	726	647.3	132.9	304.1	33.2	190.4	512.6	305.4	513.9	645	765.05	369.8	536.8	625	282.4	506
Critical Pressure, PC,bar	66.8	221.2	35	73.8	13	46	80.9	48.8	61.4	77	57.4	42.5	51.7	60.7	50.4	51.6
Critical Volume, VC,cm3/mol	2.55	57.1	93.2	93.9	65.1	99.2	118	148.3	167.1	186	228	203	219	237	130.4	192
Acentric Factor, wi	1.692718744	0.344	0.066	0.239	-0.218	0.011	0.556	0.099	0.644	0.56	0.7736	0.153	0.623	1.107	0.089	0.33
a	-5.68E+02	-2.41E+02	-1.11E+02	-3.93E+02	0.00E+00	-6.88E+01	-1.94E+02	-7.38E+01	-2.24E+02	-3.77E+02	-3.65E+02	-9.13E+01	-2.41E+02	-4.19E+02	5.86E+01	-7.85E+01
b	3.44E-01	3.51E-02	-8.65E-02	-3.21E-03	0.00E+00	3.83E-02	7.74E-02	1.01E-01	1.48E-01	2.28E-01	2.61E-01	1.71E-01	2.17E-01	3.31E-01	8.99E-03	6.04E-02
c	2.38E-04	2.02E-05	-9.63E-06	1.53E-07	0.00E+00	9.22E-05	1.16E-04	1.62E-04	1.73E-04	1.74E-04	3.11E-05	2.18E-04	2.30E-04	2.23E-04	9.82E-05	8.98E-05
d	-1.60E-07	-9.33E-09	8.56E-09	9.97E-10	0.00E+00	-5.46E-08	-7.21E-08	-1.03E-07	-1.14E-07	-1.21E-07	0.00E+00	-1.42E-07	-1.51E-07	-1.48E-07	-6.06E-08	-6.09E-08
e	3.94E-11	1.78E-12	-2.11E-12	-3.31E-13	0.00E+00	1.24E-11	1.71E-11	2.44E-11	2.76E-11	3.02E-11	0.00E+00	3.40E-11	3.66E-11	3.62E-11	1.42E-11	1.51E-11
Binary Interaction Paramater, kij																
C3H8O3	0.0000	0.3201	0.3995	0.4007	0.3414	0.4096	0.4373	0.4732	0.4916	0.5079	0.5382	0.5210	0.5323	0.5439	0.4531	0.5127
H2O	0.3201	0.0000	0.8352	0.0102	0.0007	0.0126	0.0217	0.0371	0.0467	0.0561	0.0761	0.0644	0.0720	0.0802	0.0279	0.0590
CO	0.3995	0.8352	0.0000	0.0000	0.0053	0.0002	0.0023	0.0089	0.0141	0.0197	0.0327	0.0249	0.0299	0.0355	0.0047	0.0215
CO2	0.4007	0.0102	0.0000	0.0000	0.0056	0.0001	0.0022	0.0087	0.0137	0.0192	0.0321	0.0244	0.0293	0.0349	0.0045	0.0210
H2	0.3414	0.0007	0.0053	0.0056	0.0000	0.0074	0.0146	0.0278	0.0362	0.0447	0.0629	0.0522	0.0591	0.0667	0.0199	0.0473
CH4	0.4096	0.0126	0.0002	0.0001	0.0074	0.0000	0.0013	0.0067	0.0113	0.0163	0.0284	0.0211	0.0257	0.0310	0.0031	0.0180
CH3OH	0.4373	0.0217	0.0023	0.0022	0.0146	0.0013	0.0000	0.0022	0.0050	0.0086	0.0179	0.0122	0.0158	0.0200	0.0004	0.0098
C2H6	0.4732	0.0371	0.0089	0.0087	0.0278	0.0067	0.0022	0.0000	0.0006	0.0021	0.0077	0.0041	0.0063	0.0091	0.0007	0.0028
C2H5OH	0.4916	0.0467	0.0141	0.0137	0.0362	0.0113	0.0050	0.0006	0.0000	0.0005	0.0040	0.0016	0.0030	0.0051	0.0026	0.0008
C2H6O2	0.5079	0.0561	0.0197	0.0192	0.0447	0.0163	0.0086	0.0021	0.0005	0.0000	0.0017	0.0003	0.0011	0.0024	0.0052	0.0000
C3H6O2	0.5382	0.0761	0.0327	0.0321	0.0629	0.0284	0.0179	0.0077	0.0040	0.0017	0.0000	0.0006	0.0001	0.0001	0.0129	0.0012
C3H8	0.5210	0.0644	0.0249	0.0244	0.0522	0.0211	0.0122	0.0041	0.0016	0.0003	0.0006	0.0000	0.0001	0.0010	0.0081	0.0001
C3H7OH	0.5323	0.0720	0.0299	0.0293	0.0591	0.0257	0.0158	0.0063	0.0030	0.0011	0.0001	0.0001	0.0000	0.0003	0.0111	0.0007
C3H8O2	0.5439	0.0802	0.0355	0.0349	0.0667	0.0310	0.0200	0.0091	0.0051	0.0024	0.0001	0.0010	0.0003	0.0000	0.0147	0.0018
C2H4	0.4531	0.0279	0.0047	0.0045	0.0199	0.0031	0.0004	0.0007	0.0026	0.0052	0.0129	0.0081	0.0111	0.0147	0.0000	0.0062
C3H4O	0.5127	0.0590	0.0215	0.0210	0.0473	0.0180	0.0098	0.0028	0.0008	0.0000	0.0012	0.0001	0.0007	0.0018	0.0062	0.0000

APPENDIX B

Primary Function

```
global T P Del_Gf
```

```
T0 = 298.15;
```

```
A = [3,0,1,1,0,1,1,2,2,2,3,3,3,3,2,3; 8,2,0,0,2,4,4,6,6,6,6,8,8,8,4,4;  
3,1,1,2,0,0,1,0,1,2,2,0,1,2,0,1];
```

```
Del_Gfcoeff = [-568.118,0.34354,0.00023763,-1.5973E-07,3.9424E-11;  
-240.617,0.035116,0.000020231,-9.329E-09,1.7756E-12; ...  
-110.735,-0.086474,-9.6336E-06,8.5645E-09,-2.1088E-12;  
-393.469,-0.0032129,1.5313E-07,9.9722E-10,-3.3131E-13; ...  
0,0,0,0,0; -68.772,0.03833,0.000092182,-5.4647E-08,1.2364E-11;  
-193.761,0.077372,0.00011553,-7.2147E-08,1.7054E-11; ...  
-73.783,0.10057,0.00016229,-1.0263E-07,2.4353E-11;  
-224.362,0.14774,0.00017329,-1.1358E-07,2.7577E-11; ...  
-377.018,0.22781,0.00017406,-1.2129E-07,3.0206E-11;  
-365.4610625,0.260592804,3.11083E-05,0,0; ...  
-91.273,0.1712,0.00021836,-1.4152E-07,3.4039E-11;  
-241.118,0.21677,0.00022957,-1.5085E-07,3.6621E-11; ...  
-419.406,0.33106,0.00022342,-1.4817E-07,3.6172E-11;  
58.586,0.0089877,0.00009818,-6.0588E-08,1.4246E-11; ...  
-78.507,0.060429,0.000089818,-6.0889E-08,1.5082E-11];
```

```
for P = 1:7:50
```

```
    dlmwrite('Results15.txt', P, '-append', 'roffset', 2)
```

```
    for FR = 0:0.5:5
```

```
        n0 = [1.0;FR;0.0;0.0;0.0;0.0;0.0;0.0;0.0;0.0;0.0];
```

```
        dlmwrite('Results15.txt', FR, '-append', 'roffset', 2)
```

```
    for T = 473:100:1073
```

```
        dlmwrite('Results15.txt', T, '-append', 'roffset', 2)
```

```
        Del_Gf = Del_Gfcoeff(:,1) + Del_Gfcoeff(:,2)*T +
```

```
        Del_Gfcoeff(:,3)*T^2 + Del_Gfcoeff(:,4)*T^3 +
```

```
        Del_Gfcoeff(:,5)*T^4;
```

```
        b = A*n0; lb = 1.0E-4*ones(size(n0));
```

```
        ub = 1.0E4*ones(size(n0));
```

```
        [n,fval] = fmincon(@ nG,n0,[],[],A,b,lb,ub);
```

```
        dlmwrite('Results15.txt', transpose(n), '-append', 'roffset', 1,  
        'delimiter', ' ')
```

```
        dlmwrite('Results15.txt', fval, '-append', 'roffset', 1)
```

```
    end
```

```
end
```

```
end
```

Subfunction 1

```
function f=nG(n)

global T P Del_Gf R ln_phi y A_ B_

y=n/sum(n);
ln_phi = phi_calc;
f=sum(n.*Del_Gf)+sum(n.*R*log(P))+sum(n.*R*T.*log(y))+sum(n'.*R*T.*ln_phi);
```

Subfunction 2

```
function re_val=phi_calc

global T P R y A_ B_

Tci =
[726,647.3,132.9,304.1,33.2,190.4,512.6,305.4,513.9,645,765.05,369.8,536.8,625,28
2.4,506];
Pci = [66.8,221.2,35,73.8,13,46,80.9,48.8,61.4,77,57.4,42.5,51.7,60.7,50.4,51.6];
wi = [1.692718744,0.344,0.066,0.239,-
0.218,0.011,0.556,0.099,0.644,0.56,0.7736,0.153,0.623,1.107,0.089,0.33];

ai = (0.427480233540341*R^2)*(Tci.^2)./Pci;
bi = (0.0866403499649577*R)*(Tci./Pci);
alp_i = (1+(0.48+1.574.*wi-0.176.*wi.^2).*(1-(T./Tci).^0.5)).^2;
a_alp_i = alp_i.*ai;
B_i = bi.*P/(R*T);

b = sum(y'.*bi);

kij =
[0.0000,0.3201,0.3995,0.4007,0.3414,0.4096,0.4373,0.4732,0.4916,0.5079,0.5382,0.
5210,0.5323,0.5439,0.4531,0.5127; ...
0.3201,0.0000,0.8352,0.0102,0.0007,0.0126,0.0217,0.0371,0.0467,0.0561,0.0761,0.0
644,0.0720,0.0802,0.0279,0.0590; ...
0.3995,0.8352,0.0000,0.0000,0.0053,0.0002,0.0023,0.0089,0.0141,0.0197,0.0327,0.0
249,0.0299,0.0355,0.0047,0.0215; ...
0.4007,0.0102,0.0000,0.0000,0.0056,0.0001,0.0022,0.0087,0.0137,0.0192,0.0321,0.0
244,0.0293,0.0349,0.0045,0.0210; ...
0.3414,0.0007,0.0053,0.0056,0.0000,0.0074,0.0146,0.0278,0.0362,0.0447,0.0629,0.0
522,0.0591,0.0667,0.0199,0.0473; ...
0.4096,0.0126,0.0002,0.0001,0.0074,0.0000,0.0013,0.0067,0.0113,0.0163,0.0284,0.0
211,0.0257,0.0310,0.0031,0.0180; ...
0.4373,0.0217,0.0023,0.0022,0.0146,0.0013,0.0000,0.0022,0.0050,0.0086,0.0179,0.0
122,0.0158,0.0200,0.0004,0.0098; ...
0.4732,0.0371,0.0089,0.0087,0.0278,0.0067,0.0022,0.0000,0.0006,0.0021,0.0077,0.0
041 0.0063,0.0091,0.0007,0.0028; ...
```

```

0.4916,0.0467,0.0141,0.0137,0.0362,0.0113,0.0050,0.0006,0.0000,0.0005,0.0040,0.0
016,0.0030,0.0051,0.0026,0.0008; ...
0.5079,0.0561,0.0197,0.0192,0.0447,0.0163,0.0086,0.0021,0.0005,0.0000,0.0017,0.0
003,0.0011,0.0024,0.0052,0.0000; ...
0.5382,0.0761,0.0327,0.0321,0.0629,0.0284,0.0179,0.0077,0.0040,0.0017,0.0000,0.0
006,0.0001,0.0001,0.0129,0.0012; ...
0.5210,0.0644,0.0249,0.0244,0.0522,0.0211,0.0122,0.0041,0.0016,0.0003,0.0006,0.0
000,0.0001,0.0010,0.0081,0.0001; ...
0.5323,0.0720,0.0299,0.0293,0.0591,0.0257,0.0158,0.0063,0.0030,0.0011,0.0001,0.0
001,0.0000,0.0003,0.0111,0.0007; ...
0.5439,0.0802,0.0355,0.0349,0.0667,0.0310,0.0200,0.0091,0.0051,0.0024,0.0001,0.0
010,0.0003,0.0000,0.0147,0.0018; ...
0.4531,0.0279,0.0047,0.0045,0.0199,0.0031,0.0004,0.0007,0.0026,0.0052,0.0129,0.0
081,0.0111,0.0147,0.0000,0.0062; ...
0.5127,0.0590,0.0215,0.0210,0.0473,0.0180,0.0098,0.0028,0.0008,0.0000,0.0012,0.0
001,0.0007,0.0018,0.0062,0.0000];

```

```

for i=1:16
    for j=1:16
        a_alp_ij(i,j)=y(i)*((1-kij(i,j))*sqrt(a_alp_i(i)*a_alp_i(j)));
    end
    a_alp_ij(i,:)=a_alp_ij(i,:).*y(i);
end

```

```

a_alp=sum(sum(a_alp_ij));
A_=a_alp*P^2/(R*T)^2;
B_=b*P/(R*T);

```

```

%-----

```

```

Z = fzero(@f_Z,0.0001)

```

```

ln_phie=(B_i/B_)*(Z-1)-log(Z-B_)+(A_/B_)*(B_i/B_-
2/a_alp.*sum(a_alp_ij)./y')*log(1+B_/Z);

```

```

re_val=ln_phie;

```

Subfunction 3

```

function u = f_Z(z)

```

```

global A_ B_

```

```

u = z^3-z^2+(A_-B_-B_^2)*z-A_*B_;

```